LOADS TECHNOLOGY FOR SUPERSONIC CRUISE AIRCRAFT

Robert C. Goetz
Langley Research Center

SUMMARY

A SCAR Loads Technology Program was initiated in 1973 and includes research in aeroelastic loads, landing loads, acoustic loads, and the measurement of atmospheric turbulence. This paper presents the current status and some results obtained to date for the latter three research areas.

Specifically, a flight program to measure atmospheric turbulence at high altitudes (long wavelengths) in a variety of meteorological conditions is described and some results obtained in high-altitude wind shear are discussed. Results are also presented from wind-tunnel test programs to measure fluctuating pressures associated with over-the-wing engine configurations. Two analyses, a flexible aircraft take-off and landing analysis and an active control landing-gear analysis, have been developed and their capabilities are described. Efforts to validate these analyses with experimental data are also discussed as well as results obtained from parametric studies.

INTRODUCTION

Efficient structural design of a supersonic cruise aircraft is predicated by the accurate knowledge of the critical design loads. Earlier design studies (ref. 1) have indicated the types of critical flight and ground load conditions for the design of typical supersonic cruise aircraft structure and control systems. It was apparent that the critical design conditions for most of the aircraft structure occurred in the transonic speed regime. Critical conditions included balanced maneuvers, abrupt maneuvers, and gusts. Unfortunately, the load prediction methodology is least reliable in this speed regime. Additionally, for high-speed flight, the slender more flexible configurations require more emphasis on landing loads and response, aeroelastic effects, dynamic response to atmospheric turbulence, and fatigue life considerations.

Consequently, a loads program was undertaken to provide an expanded technology which will permit more efficient supersonic cruise aircraft structural design by improved loads and aeroelastic predictive methodology. The SCAR Loads Technology Program is comprised of four elements which include research in aeroelastic loads, landing loads, acoustic loads, and the measurement of atmospheric turbulence. The long range goal of each of these areas is to provide aeroelastic load prediction methodology, develop and validate a take-off and landing analysis including aircraft flexibility and active landing gear design methodology, improved fatigue life prediction methodology, and

to provide a description of the high altitude turbulence environment in a wide variety of meteorological conditions for improved gust-loads prediction methodology, respectively. A review of the aeroelastic loads element is given in references 2 to 6. This paper will discuss the remaining three program elements and present the current status and summarize some results obtained to date.

ATMOSPHERIC TURBULENCE

A number of earlier programs have been devoted to measurements of atmospheric turbulence. Results from these programs have, in general, yielded the conclusion that the von Karman description of atmospheric turbulence spectra is valid for the slope of the power spectrum (-5/3) at reduced frequencies above about 10^{-3} cycles/m. In the von Karman equation (shown in fig. 1), a value L essentially defines the location of the "knee" in a curve of power spectral density Φ against frequency and thus if σ, the root mean square or intensity level, and L are known, the power spectrum is completely defined. Limitations in both instrumentation and data reduction procedures prevented acquiring data at wavelengths long enough to identify appropriate values of L for the von Karman equation. An example of the significance of the L value for aircraft designers is shown by the vertical bands in figure 1. The primary aircraft response to turbulence is in the rigid body, short period, and Dutch roll modes. For subsonic aircraft such as the 707, B-52, and 747 airplanes which cruise at Mach 0.8 and at altitudes, h, of 11 to 12 km (35 000 to 40 000 ft), the primary response to turbulence is to the right of the knee of the spectral curves for all values of L in the range believed appropriate for consideration. However, for supersonic cruise aircraft, that is, cruise at Mach 2.7 at an altitude of approximately 18 km (60 000 ft), the predicted response is more significantly affected by the L value as can be seen in the figure. Fatigue and ride quality are also important aspects of the aircraft response to atmospheric turbulence. Consequently, a flight measurement program was initiated to determine whether the von Karman equation is appropriate to represent turbulence at the high altitudes (long wavelengths) in various meteorological conditions, and, if so, to define the appropriate L values.

Measurement of Atmospheric Turbulence

The Measurement of Atmospheric Turbulence (MAT) program, being conducted by the Langley Research Center in cooperation with the Dryden Flight Research and Johnson Space Centers, was established to measure all three components of turbulence (vertical, lateral, and longitudinal) over a wide altitude range in different meteorological conditions. It was decided that two sampling aircraft would be required for measurements over the entire range of interest — one airplane covering the range from sea level to 15 km (50 000 ft) altitude and a special high altitude airplane for altitudes above 15 km. The sensors selected required sampling to be done at subsonic

speeds. A B-57B Canberra shown in figure 2 was selected for the sampling up to 15 km and it was decided that a B-57F would be the preferred aircraft for use above 15 km.

The basic measurements of vertical and lateral turbulence components are made by utilizing lightweight balsa vanes mounted on a stiff nose boom. Aircraft motion corrections are accomplished by using onboard inertial platform and rate gyros. The longitudinal turbulence component is made by utilizing a specially designed instrument measuring small pressure fluctuations superimposed on a relatively large nominal pressure. Incremental static pressure is recorded in addition to incremental total pressure in order to be able to account for changes in total pressure which result from airplane altitude variations during a data acquisition period of the flight test.

The equations used for determining time histories of gust velocity are given in reference 7. To obtain power estimates at the extremely low frequencies required (i.e., long wavelengths), narrow spectral "windows" (bandwidths) on the order of 0.02 Hz must be used in the data processing procedure. Such narrow spectral windows introduce wild statistical fluctuations in the power estimates unless relatively long data samples can be obtained. The statistical reliability believed necessary requires on the order of 24 to 30 statistical degrees of freedom for the spectral values, which translates to data samples of at least 10 minutes duration. Details concerning the power spectral algorithms employed, and the justification for not prewhitening the time histories for long wavelength analysis are given in reference 8. Instrumentation details and measurement accuracies are given in reference 9. An assessment of the overall instrumentation performance by means of inflight maneuvers, together with assessment of possible low frequency trend-type errors based upon post-flight performance of the inertial platform system, is given in reference 10. A unique feature of this program is the fact that the same instrumentation and data reduction procedure is employed for all measurements covering altitudes from near sea level to about 18 km (60 000 ft) and the various meteorological conditions.

Sampling flights with the B-57B were made in the March 1974 to September 1975 time period. A total of 46 flights were made, 30 in Eastern U.S. within range of the airplane based at Langley AFB, VA, and 16 in Western U.S. within range of the airplane based at Edwards AFB, CA. A full-time project meteorologist provided functions of coordinating and planning flights, observing from the rear seat during the flights, and conducting post-flight analyses to document pertinent meteorological parameters and to define the meteorological condition where turbulence was encountered.

A summary of data obtained is given in table I with the number of data runs to be processed associated with six meteorological conditions. Data processing is currently under way. A typical sample of turbulence categorized as high-altitude wind shear, which is a predominate type of encounter expected for high-altitude supersonic cruise aircraft, will be discussed.

High-Altitude Wind Shear Result

The time histories for the high-altitude wind shear case are presented in figure 3. The intensity of the turbulence for all three components u,

v, and w is gradually increasing with time. Such nonhomogeneous (or nonstationary) behavior has generally been believed to be responsible for considerable rounding or smoothing of the spectral knee. The recent work of reference 11, however, indicates that unless the change in intensity is considerably more abrupt than shown here, little effect should be observable in the spectra. It is obvious that significant low frequency power is present in the horizontal components. This is assumed to be directly attributable to the changing horizontal wind field. The low frequency content can be thought of as a modulation of the mean value with a typical high-frequency amplitude-modulated random process superimposed. (A model of turbulence which includes mean modulation has been suggested by Reeves, et al. in ref. 12.) No pronounced low frequency power is noted in the vertical component. These observations are substantiated in the corresponding power spectra shown in figure 4.

The power spectra curves presented in figure 4 are comparable with those of figure 1 except that the results have not been normalized; i.e., the area under the curve is equal to the variances, or σ^2. The abscissa values were obtained by converting Hz to inverse wavelength by using the average true airspeed for each data run of the flight test. Superimposed on the data are shown theoretical von Karman type curves with selected L values. Note that the slopes of the curves match at the higher frequencies. Although an L value of 300 m (1000 ft) appears to be appropriate for the vertical component, L values of greater than 1800 m (6000 ft) would apply for the horizontal components directly reflecting the large power content at low frequencies. Additional data from this program are presented and discussed by Rhyne, et al. for terrain-related rotor, thermal convective, and mountain wave turbulence cases in reference 13.

Presently, a B-57F aircraft is being modified to accept the MAT instrumentation system and sampling flights above 15 km (50 000 ft) are scheduled during the first part of 1977.

ACOUSTIC LOADS

Supersonic cruise aircraft configurations with engines located over the wing and forward have been proposed to obtain increased lift for low speed flight, decreased ground noise by wing shielding, improved flutter behavior, and improved center-of-gravity locations. Location of the engines over the wings has the disadvantage of exposing the fuselage and wing upper surface to intense fluctuating pressures from the high-velocity engine exhaust. Acoustic fatigue and excessive cabin noise may then be difficult to prevent. In order to provide information on the fluctuating pressures, several small-scale model investigations have been conducted.

Test Program

Figure 5 indicates two of the models tested. The model on the left was used by Willis in an investigation conducted in the Langley anechoic facility. The model was a 0.03-scale planform of the SCAT-15. The jet was a Mach 1.5,

fully expanded, convergent-divergent nozzle operating on cold air and at zero forward speed. The jet exit was located near the wing leading edge, one exit diameter above the wing surface and directed 3° downward toward the wing surface. The model on the right has a Mach 1.4 plug nozzle and is currently being tested statically and with forward velocity to determine the effects of engine location and engine exhaust impingement angle on the resulting fluctuating pressure loads on the wing surface.

Results

Figure 6 shows fluctuating pressure loadings measured on the SCAT-15 wing with the M = 1.5 engine model. Also shown on the figure are calculated loadings for the same engine model mounted beneath the wing at the trailing edge. These noise loading contours were calculated using AGARD design data charts. The maximum 130 dB loadings for the trailing edge engine location is below the predicted levels that would be generated by a supersonic boundary layer and therefore of little interest to the designer. However, the 167 dB loading with the over-the-wing location is high; therefore, design attention will be required to provide a reasonable fatigue-life design and it also suggests that additional design attention will be required to achieve acceptable cabin noise levels. The jet velocity for this test was about 440 m/s; current considerations are for supersonic jets having velocities of 845 m/s. Therefore, scaling the data to this higher velocity by using a semiempirical method in reference 14 indicates a maximum level for the scaled loads of 181 dB. Figure 7 shows a sample one-third-octave spectrum of measured data that has been scaled to full-scale aircraft frequency, a jet velocity of 845 m/s, and corrected to cruise altitude density. The levels shown for the 50 to 1000 Hz range usually considered in fatigue life design are high enough to indicate that a serious penalty is incurred for over-the-wing engine location if a high velocity engine is used.

LANDING LOADS

Dynamic loads in aircraft resulting from the landing impact phase and the rollout and take-off phases of aircraft operations on rough runways, are recognized as significant in contributing to structural fatigue. In addition, the associated induced vibrations contribute to ground handling problems and crew and passenger discomfort. Such vibration problems have been encountered with conventional transport aircraft and have required modifications to the landing gear systems to improve ride and handling qualities subsequent to the aircraft's entry into service. Ground-induced dynamic loads and vibrations and the resulting problems will be magnified for supersonic cruise aircraft because of the increased structural flexibility of the slender-body, thin-wing configuration and the higher take-off and landing speeds. Consequently, an accurate prediction of the ground-induced loads and vibrations and a method for alleviating excessive loads and motions applied to the airframe are needed. The application of active control landing-gear systems in the design of supersonic cruise aircraft could help to alleviate these dynamic loads and vibrations and provide the aircraft with longer operational

life, safer ground handling characteristics, and more acceptable ride quality.

Active control systems have been applied to ground vehicle suspension systems and are being extensively investigated for application to aircraft aerodynamic controls. Some analytical studies have also been conducted to determine the feasibility of applying active controls to aircraft landing-gear systems. These studies have been primarily concerned with the rollout or taxiing modes of aircraft operations. There is a dearth of information available, however, for actively controlling loads transmitted to the airframe by the landing gear during the impact phase, and no published information is available containing experimental data on actively controlled landing gears.

Experimental and analytical research and development is being conducted by McGehee and Carden of the Langley Research Center to obtain accurate predictions of ground-induced loads and vibrations and to develop the design methodology for active control landing-gear concepts. This section of the paper will describe the prediction methods developed, the validation results to date through comparison with experiment, and planned work in this area.

Flexible Aircraft Take-off and Landing Analysis (FATOLA)

Improved prediction of the airframe structural response is being accomplished with an analysis called FATOLA which provides a comprehensive simulation of the aircraft take-off and landing modes. As illustrated in figure 8, impact loads, runway induced loads, steering loads, perturbation or operational loads (including thrust reversal, braking, aerodynamic loads and asymmetric impact capability) and airframe flexibility characteristics, are combined to make up the total aircraft response analysis. Basically, the analysis can simulate an aircraft either as a six-degree-of-freedom rigid body or as a flexible body over a flat planet. In the flexible body option, the airframe flexibility is represented by the superposition of from one to 20 free-free vibratory modes (input to the program) on the rigid body motions. In the rigid body option, comprehensive information on the airframe, state of maneuver logic, autopilots and control response, and dynamics of the landing gears are output. In the flexible body option, elastic body and total (rigid body plus elastic body) displacements, velocities, and accelerations at up to 20 points on the aircraft are also obtained. Complete details of the computer program are given in references 15 and 16.

Rigid body simulation for X-24B vehicle.- To verify the simulation capabilities of the FATOLA computer program rigid body option, the X-24B manned lifting body research vehicle was selected since unpublished experimental landing loads and motions data were available for this vehicle. As shown in figure 9, this vehicle is delta-shaped with blended wings and a flat bottom. The X-24B was used in a joint NASA/USAF flight research program to explore the subsonic to low supersonic performance characteristics with emphasis on the landing maneuver.

Flight test data from an asymmetric landing of the X-24B were selected for the X-24B simulation study. Pertinent touchdown parameters for the unpowered X-24B landing were: a sink rate of 0.49 m/s (1.6 fps); a ground speed of 87.1 m/s (286 fps); a pitch angle of 13.4° with a nose-over pitch rate of -0.8°/sec; a roll angle of 2° right with a 4.4°/sec right roll rate. The landing surface was assumed to be flat since the actual landing surface inclination and perturbations were undefined.

Typical analytical vertical loads and the associated gear strokes predicted by using the rigid body option of FATOLA are compared with experimental flight test data in figure 10. In figure 10, the results for the right main and nose gears show that the levels of load generally compare well throughout the first 3.5 seconds of impact and rollout time history. However, the predicted loads indicate a slightly higher initial peak and a slighly lower second peak for the main gear as compared with the experimental data. Also included in figure 10 are the analytical and experimental time histories of gear strut stroke for the right main and nose gears. The overall agreement of both magnitude and variation with time between the predicted strut strokes and flight test data is excellent. Comparison of other parameters such as pitch rate, etc. can be found in reference 16.

Flexible body simulation for YF-12 aircraft.- The aircraft used to validate the capabilities of the FATOLA flexible body option and to verify the analysis was the YF-12 aircraft shown in figure 11. This aircraft has a modified delta wing planform and is powered by two jet engines. This fully instrumented, large, flexible, supersonic research vehicle was used in a joint DFRC/LaRC landing loads and motions program recently completed at the Dryden Flight Research Center (DFRC).

The flexibility of the aircraft was represented with the first 10 modes available from a two-dimensional finite-element representation of an aircraft in the YF-12 series. The flexible modes are only generic for the YF-12 class of aircraft and have just vertical modal deflections; they are limited in the wing directions to symmetric modes. Work is currently underway to obtain both symmetric and antisymmetric modal data from a three-dimensional finite-element model of the specific test aircraft for which landing data have been obtained.

Flight test data for an asymmetric landing of the YF-12 aircraft were also selected for the YF-12 simulation study. The touchdown parameters for the flight were: a sink rate of 0.305 m/s (1.0 fps); a pitch angle of 8.3° with a nose-over pitch rate of -0.2°/sec; and a roll angle of 1.2° right. The landing surface was the Edwards Air Force Base runway and the surface perturbations as a function of runway distance were measured prior to the test program.

Typical predictions of the YF-12 aircraft nose gear vertical load are presented in figure 12. Predictions using the rigid body option indicate three almost complete unloadings with six major peaks between 6-1/2 and 10 seconds in time. However, using the flexibility option altered the predicted load pattern to only four major peaks over the same time span. Comparison of the flexible prediction with flight test data indicates excellent agreement in magnitude and

loading pattern and illustrates the importance of structural flexibility in altering the loading behavior of this type of aircraft. Good correlation was also obtained for structural accelerations along the body of the aircraft, as well as for other parameters.

Active Control Landing Gear Analysis (ACOLAG)

An analysis has been developed for the study of actively controlled landing-gear systems. This analysis considers the following parameters shown in figure 13: sinusoidal or random runway roughness; empirical tire-force deflection characteristics; automatic (anti-skid) braking; oleo-pneumatic strut with fit and binding friction; closed-loop, series-hydraulic control with feedback; first-mode wing bending and torsional structural elastic characteristics; and theoretical subsonic aerodynamics. This model has been validated for conventional (passive) gears by comparing calculated results with experimental data obtained from vertical drop tests in reference 17.

The shock strut force computed by using the active control landing gear analysis, for a passive gear, is in good agreement with the experimental data (within the accuracy limits cited for the experimental shock strut force of ±2.224 kN (±500 lbf). Other comparisons of computed and experimental ground forces and the relative motions of the airplane and gear show as good or better agreement as that shown for the shock strut forces. The active control landing-gear analysis is, therefore, valid for predicing landing loads and motions of an airplane during symmetric impact or rollout.

A study has been conducted for the series-hydraulic control gear concept shown in figure 14. This gear employs a hydraulic control actuator in series with a simply modified version (modified orifice tube and strut static extension) of a passive gear from a 2721.6 kg (6000 lb) class general aviation aircraft.

Figure 15 presents computed results from landing impact and rollout simulations of passive and modified version active gears. As shown on the figure, the active control gear reduced the wing force by 18 percent during the initial landing impact and 80 percent during secondary impact of the main gear, due to nose gear impact and rollout, and required an increase in strut stroke of 25 percent. If an aluminum wing structure with a full-reversed stress of 269 MPa (39 000 psi) is assumed when employing the passive gear, the fatigue life would be approximately 20 000 cycles. For the aluminum wing structure, the 18-percent reduction in wing force would correspond to a fatigue life of 54 000 cycles, a factor of approximately 2.7 times that of the passive gear accounting only for the impact phase. The maximum control flow rates required during this simulation were 0.31 m^3 (83 gallons) per minute for removal of fluid from the strut and 0.23 m^3 (60 gallons) per minute for the addition of fluid to the strut.

Presently, a passive gear shown in figure 16 is undergoing modifications and the active control electronic system is being designed and fabricated so that these analytically predicted results can be verified through testing at the NASA Langley landing loads track. The actively controlled gear system will subsequently be tested on a full-scale general aviation aircraft to further demonstrate the concept. Concurrent with the experimental effort, another active control gear concept which has the control installed parallel with the shock strut is being analytically investigated.

In addition, the FATOLA computer program is being modified to include ACOLAG; and thus provide a valid, comprehensive, multi-degree-of-freedom landing and take-off analysis for use in the study and design of landing-gear systems for supersonic cruise aircraft.

CONCLUDING REMARKS

Since the SCAR Loads Technology Program was initiated in 1973, accomplishments to date and results in three of the program areas discussed in this paper are as follows:

(1) Measurement of atmospheric turbulence: Data have been collected from 46 flights for 76 turbulence encounters between 0.3 and 15 km (1000 and 50,000 ft) altitude. The associated meteorological conditions have been identified. The most prevalent meteorological condition for turbulence encountered was the high-altitude wind shear and for this case the following observations are made:

(a) For all encounters, the -5/3 slope of the von Karman turbulence model over the short wavelength region was experimentally confirmed.

(b) The von Karman turbulence model also appears to be appropriate for the <u>vertical</u> component at the longer wavelengths with an integral scale value of 300 m (L = 1000 ft).

(c) However, for the <u>horizontal</u> components, the very large power obtained at the long wavelengths makes it doubtful whether the von Karman model is applicable in this region. If it is, integral scale values greater than 1800 m (L > 6000 ft) are required.

Results from this program should assist in clarifying the nature of the power content of atmospheric turbulence at low frequencies (long wavelengths), and will aid designers of supersonic cruise aircraft.

(2) Acoustic loads: Small-scale static model tests have been conducted on over-the-wing engine configurations to measure fluctuating surface pressures in the jet exhaust impingement area. Variables tested include jet exit Mach number, nozzle deflection angle, engine location above the wing and spanwise and chordwise placement. Results indicate that overall sound pressure levels (OASPL) greater than 160 dB occur in the jet impingement area over large regions of the model surface. These overall levels when extrapolated to full-scale values are high enough to require considerable attention in the design of a wing to achieve acceptable acoustic fatigue lifetime.

(3) Landing loads: A flexible aircraft take-off and landing analysis (FATOLA) has been developed and correlations between X-24B and YF-12 flight test data and analytical results indicate that the analysis is a valid and versatile tool for the study of landing loads and motions of aircraft.

An active control landing gear analysis (ACOLAG) has been developed and verified for passive, conventional landing-gear systems. Parametric studies for a series-hydraulic active control gear concept using ACOLAG indicate the feasibility of the concept and potential load alleviations during the landing phase are shown to improve aircraft fatigue life, ground handling and crew and passenger comfort. Experimental full-scale tests using a series-hydraulic active control gear system are to be performed to validate ACOLAG, and other active control gear concepts are being analytically evaluated. Once ACOLAG has been validated, it is planned to combine this capability into FATOLA.

REFERENCES

1. Manro, M. E.; Moulijn, J. P.; and Knittel, J. D.: SST Technology Follow-On Program - Phase I: Pre-sure Distributions on a Delta Wing Horizontal Stabilizer Combination at Mach Numbers from 0.3 to 2.9 - Volume 1 Summary Report. FAA-SS-72-30-1, July 15, 1972.

2. Manro, M. E.; Tinoco, E. N.; and Bobbitt, P. J.: Comparisons of Theoretical and Experimental Pressure Distributions on an Arrow-Wing Configuration at Transonic Speeds. NASA SP-347, 1975.

3. Manro, M. E.; Manning, K. J. R.; Hallstaff, T. H.; and Rogers, J. T.: Transonic Pressure Measurements and Comparison of Theory to Experiment for an Arrow-Wing Configuration - Summary Report. NASA CR-2610, 1975.

4. Manro, M. E.; Bobbitt, P. J.; and Rogers, J. T.: Comparisons of Theoretical and Experimental Pressure Distributions on an Arrow-Wing Configuration at Subsonic, Transonic, and Supersonic Speeds. AGARD Fluid Dynamics Panel Symposium, Moffett Field, CA, September 27-29, 1976. AGARD Preprint 204.

5. Bobbitt, Percy J.; and Manro, Marjorie E.: Theoretical and Experimental Pressure Distributions for a 71.2° Swept Arrow-Wing Configuration at Subsonic, Transonic, and Supersonic Speeds. Proceedings of the SCAR Conference, NASA CP-001, 1977. (Paper no. 5 of this compilation.)

6. Murrow, H. N.; and Rhyne, R. H.: The MAT Project - Atmospheric Turbulence Measurements with Emphasis on Long Wavelengths. Proceedings of the 6th Conference on Aerospace and Aeronautical Meteorology, American Meteorological Society (El Paso, TX), November, 1976, pp. 313-316.

7. Keisler, S. R.; and Rhyne, R. H.: An Assessment of Prewhitening in Estimating Power Spectra of Atmospheric Turbulence at Long Wavelengths. NASA TN D-8288, 1976.

8. Meissner, C. W., Jr.: A Flight Instrumentation System for the Acquisition of Atmospheric Turbulence Data. NASA TN D-8314, 1976.

9. Rhyne, R. H.: Flight Assessment of Atmospheric Turbulence Measurement System with Emphasis on Long Wavelengths. NASA TN D-8315, 1976.

10. Mark, W. D.; and Fisher, R. W.: Investigation of the Effects as Nonhomogeneous (or Nonstationary) Behavior on the Spectra of Atmospheric Turbulence. NASA CR-2945, 1976.

11. Reeves, P. M.; Joppa, R. G.; and Ganzer, V. M.: A Non-Gaussian Model of Continuous Atmospheric Turbulence Proposed for Use in Aircraft Design. NASA CR-2639, 1976.

12. Rhyne, R. H.; Murrow, H. N.; and Sidwell, K. W.: Atmospheric Turbulence Power Spectral Measurements to Long Wavelengths for Several Meteorological Conditions. Aircraft Safety and Operating Problems, NASA SP-416, 1976, pp. 271-286.

13. Guinn, W. A.; Balena, F. J.; Clark, L. R.; and Willis, C. M.: Reduction of Supersonic Jet Noise by Over-the-Wing Engine Installation. NASA CR-132619, April 1975.

14. Guinn, W. A.; Balena, F. J.; and Soovere, J.: Sonic Environment of Aircraft Structure Immersed in a Supersonic Jet Flow Stream. NASA CR-144996, June 1976.

15. Dick J. W.; and Benda, B. J.: Addition of Flexible Body Options to TOLA Computer Program. NASA CR-132732, September 1975.

16. Carden, H. D.; and McGehee, J. R.: Validation of FATOLA Computer Program Using Flight Landing Data. AIAA Paper No. 77-404, Mar. 1977.

17. McGehee, J. R.; and Carden, H. D.: A Mathematical Model of an Active Control Landing Gear for Load Control During Impact and Rollout. NASA TN D-8080, January 1976.

TABLE I.- SAMPLING SUMMARY OF B-57B FLIGHTS

[46 FLIGHTS WERE MADE BETWEEN MARCH 1974 AND SEPT. 1975]

(30 EASTERN U.S. AND 16 WESTERN U.S.)

TURBULENCE CATEGORY	NUMBER OF DATA RUNS
TERRAIN RELATED, ROTOR	14 (6 FLIGHTS)
THERMAL , CONVECTIVE	8 (2 FLIGHTS)
NEAR THUNDERSTORMS	12 (2 FLIGHTS)
JET STREAM AND HIGH-ALTITUDE WIND SHEAR*	27 (6 FLIGHTS)
MOUNTAIN WAVES	8 (4 FLIGHTS)
ISOLATED SITUATIONS	7 (2 FLIGHTS)

* CASE SELECTED FOR REVIEW IN THIS PAPER

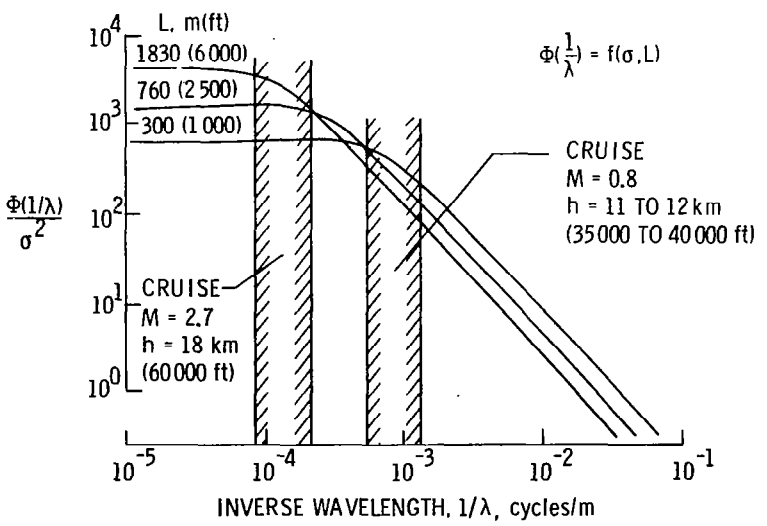

Figure 1.- Theoretical power spectra. Von Karman turbulence model.

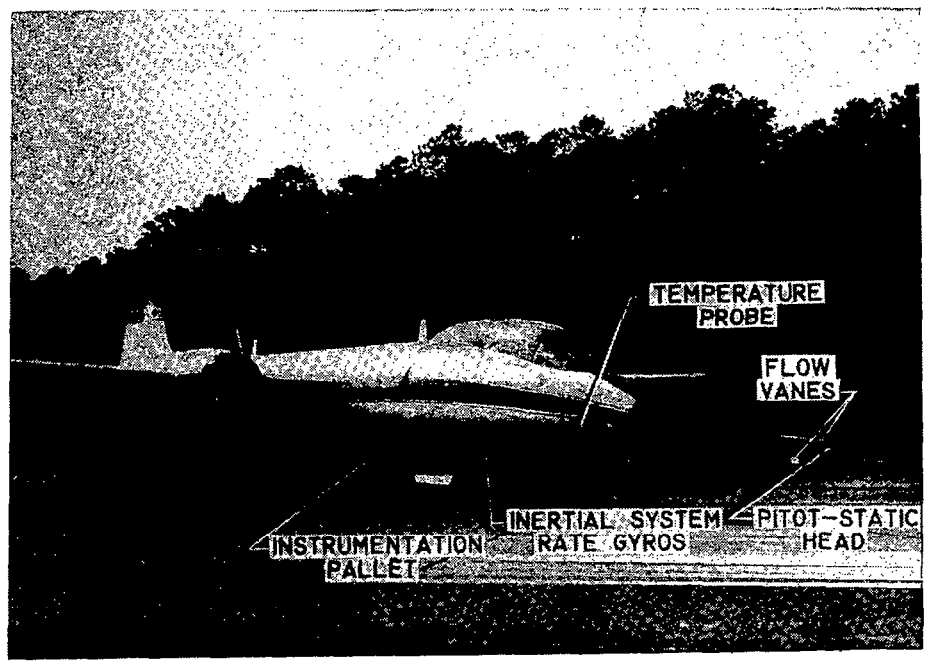

Figure 2.- B-57B instrumented airplane.

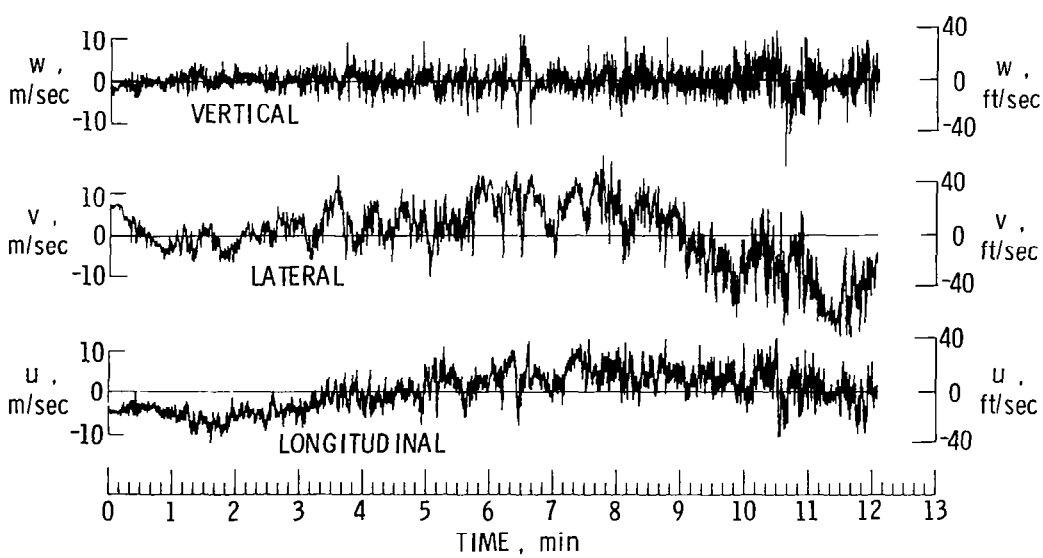

Figure 3.- Turbulence time histories. High altitude wind shear.

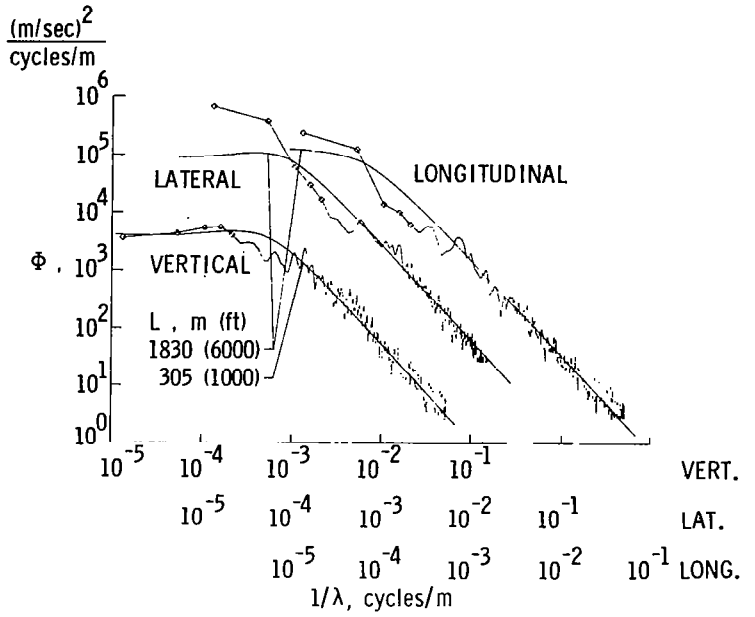

Figure 4.- Power spectral density. High altitude wind shear.

M = 1.5 convergent-divergent nozzle M = 1.4 nozzle

Figure 5.- Acoustic model tests on over-the-wing engine configurations.

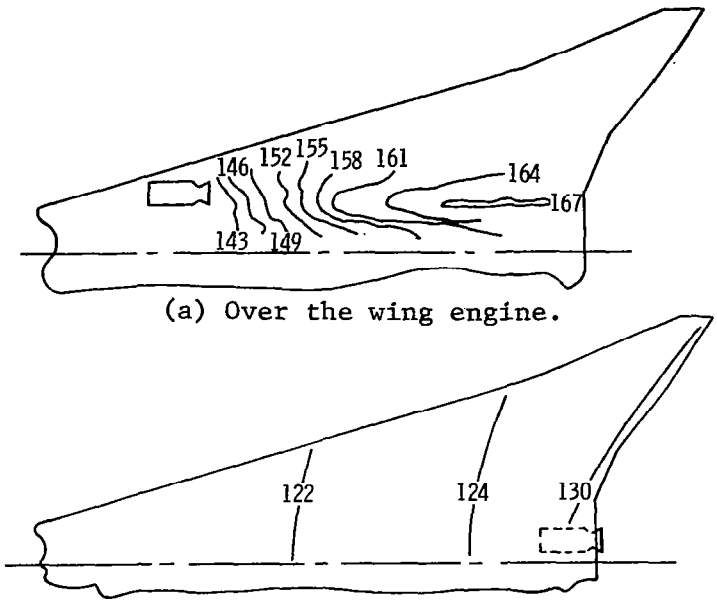

(a) Over the wing engine.

(b) Under the wing engine.

Figure 6.- Fluctuating pressure contours, dB.

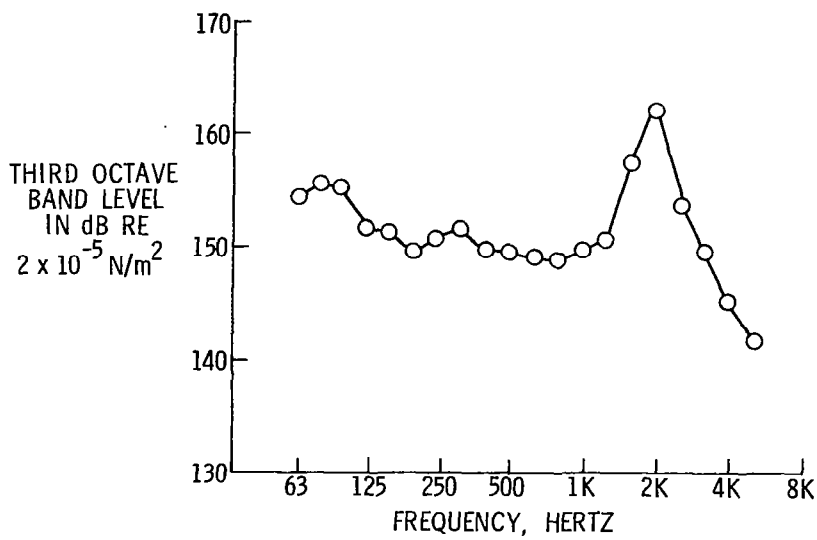

Figure 7.- Full-scale spectrum of measured data.

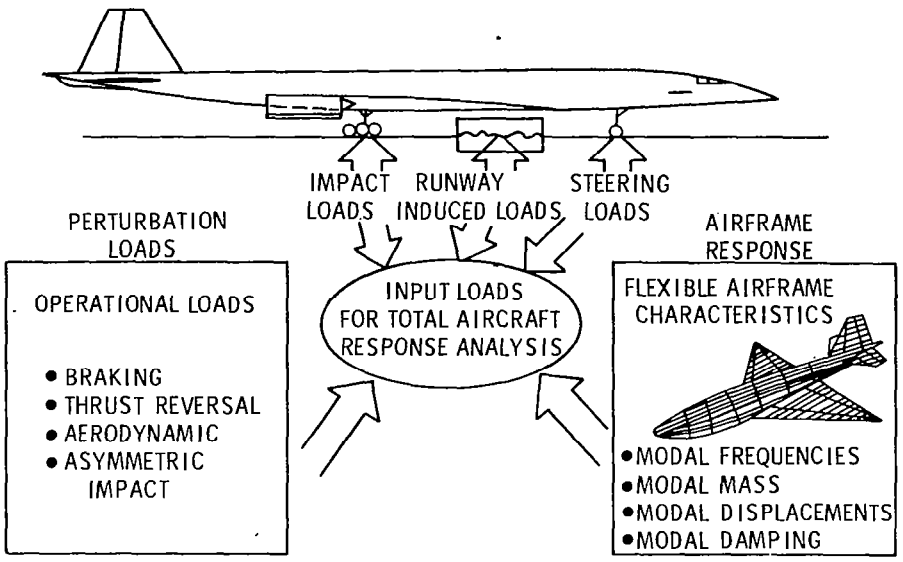

Figure 8.- Flexible aircraft take-off and landing analysis (FATOLA).

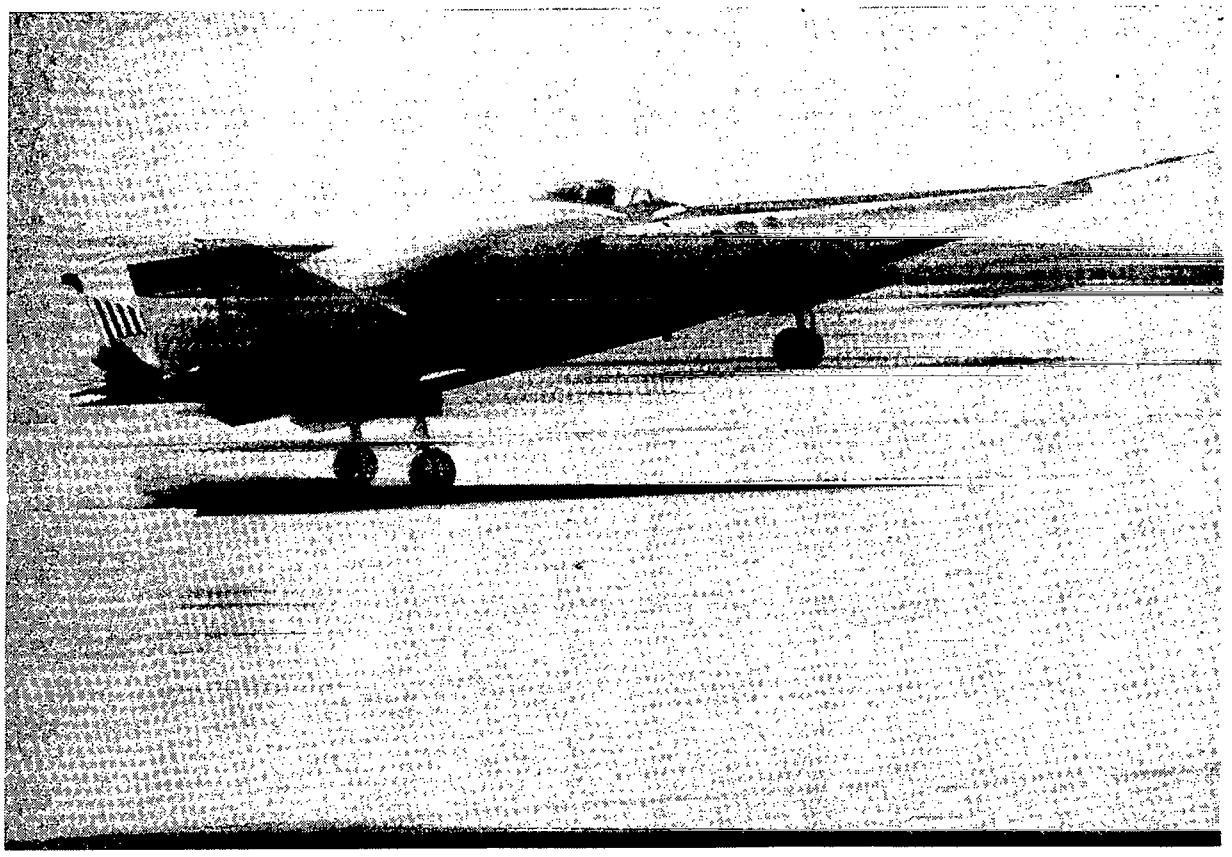

Figure 9.- X-24B landing flight test.

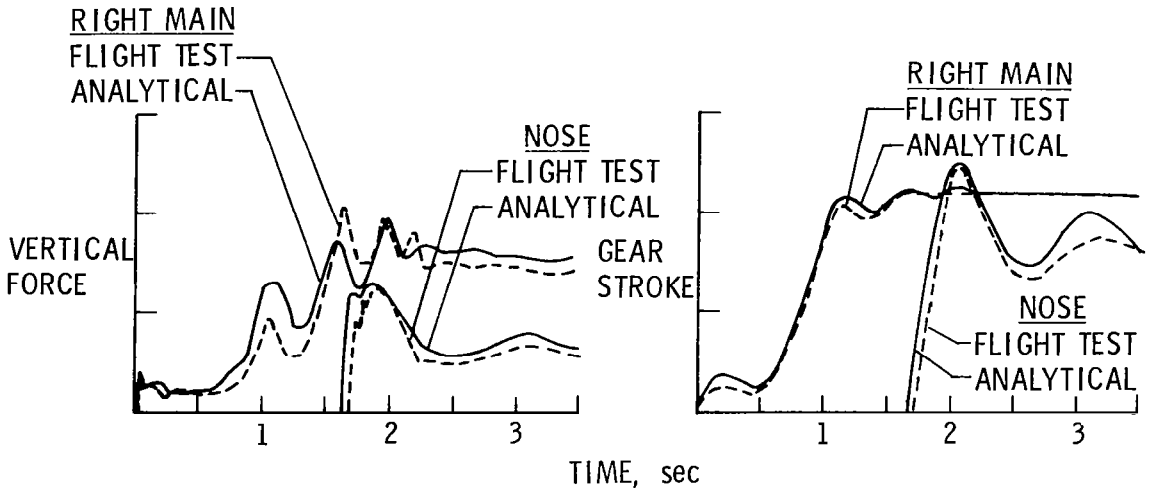

Figure 10.- X-24B experimental compared with analytical results.

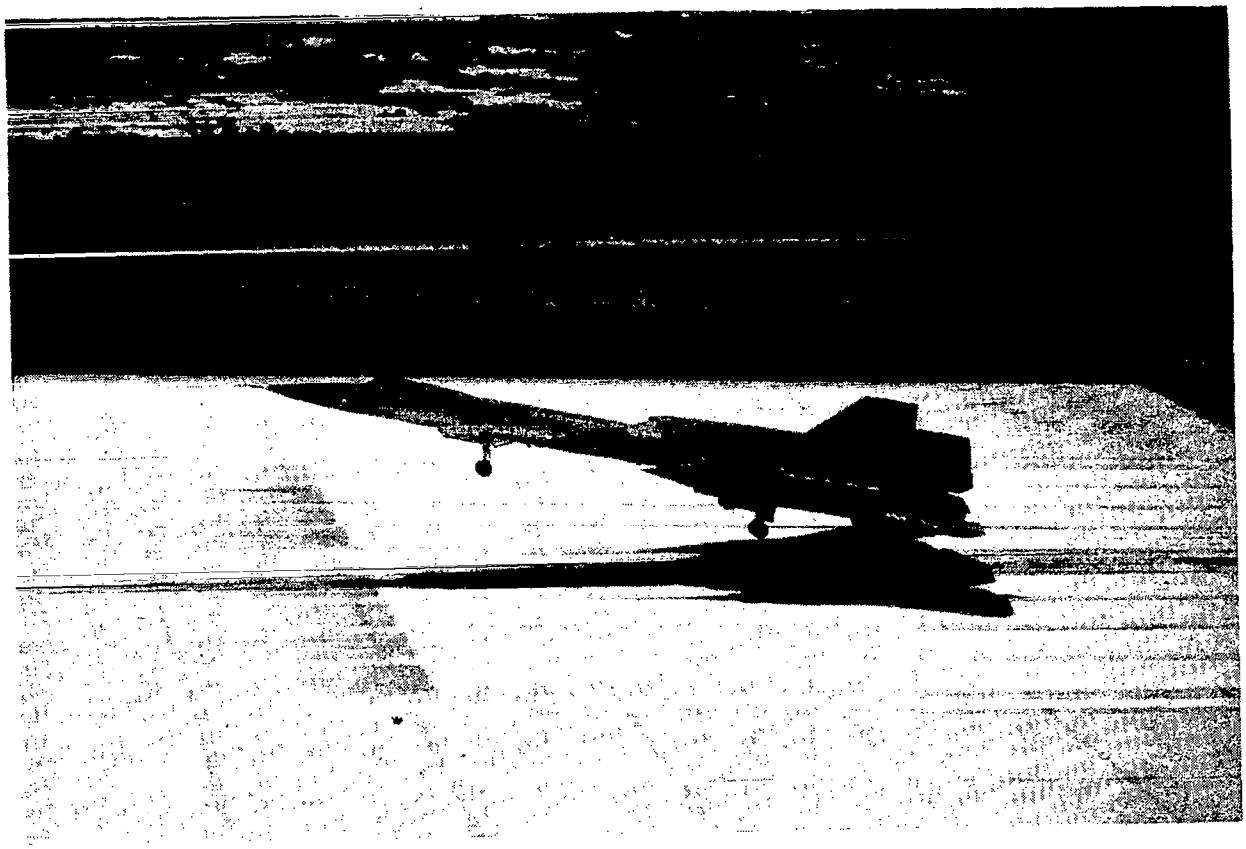

Figure 11.- YF-12 landing flight test.

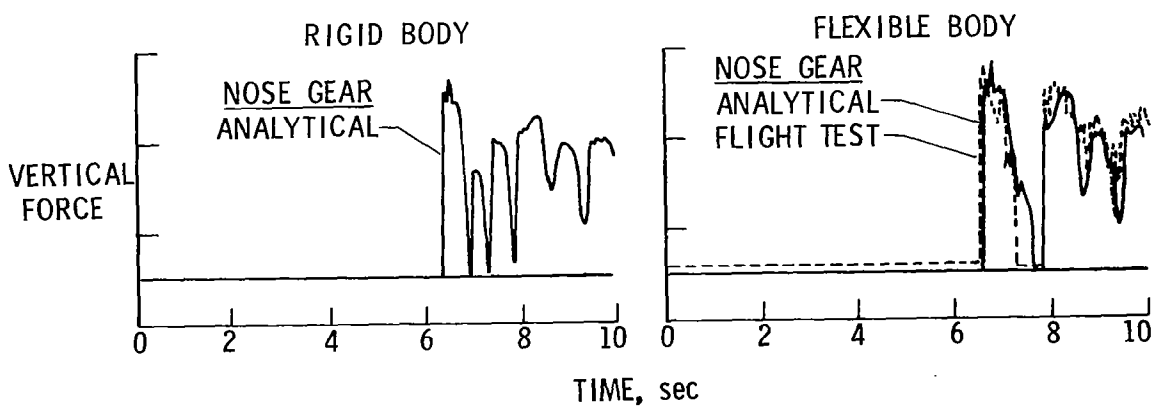

Figure 12.- YF-12 experimental compared with analytical results.

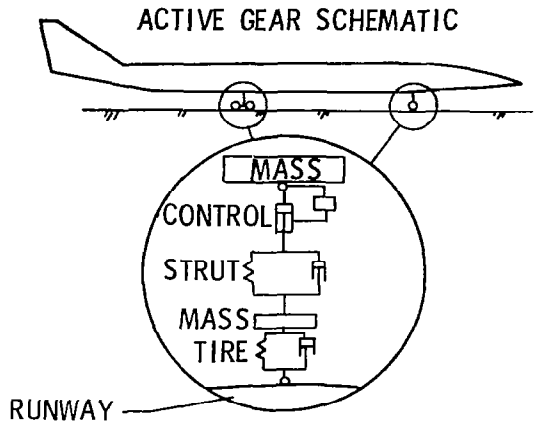

ANALYTICAL CAPABILITIES
RUNWAY UNEVENNESS
NONLINEAR TIRE FORCES AND ANTI-SKID BRAKING
OLEO-PNEUMATIC STRUT WITH FRICTION
CLOSED-LOOP, SERIES-HYDRAULIC CONTROL
FIRST MODE WING BENDING AND TORSION
THEORETICAL SUBSONIC AERODYNAMICS

Figure 13.- Active control landing-gear analysis (ACOLAG).

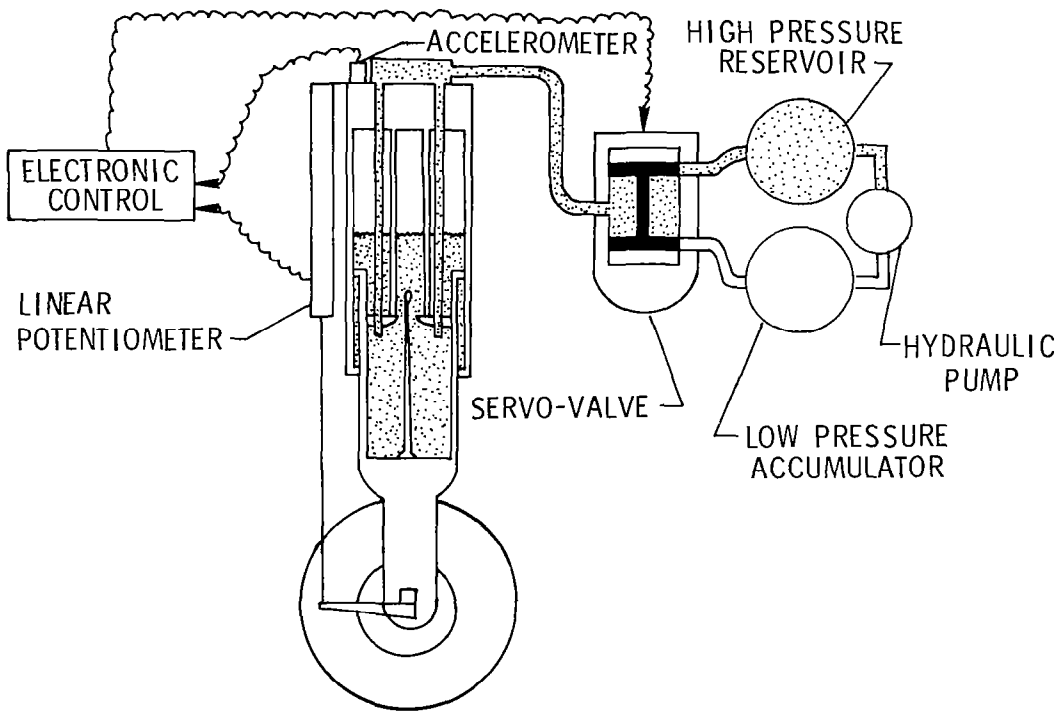

Figure 14.- Series-hydraulic active control concept.

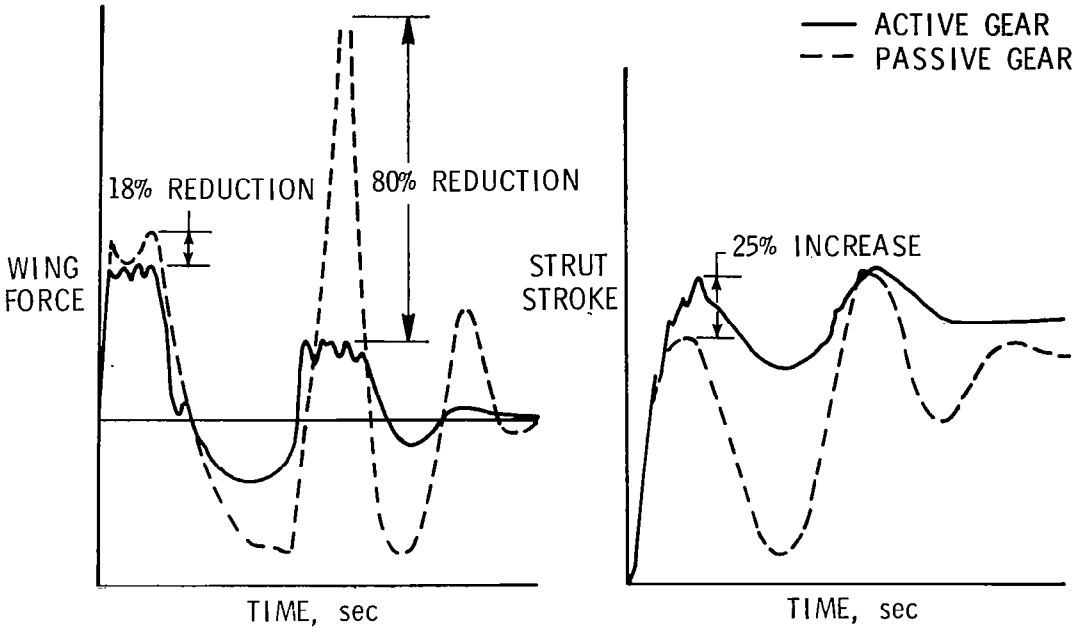

Figure 15.- Analytical results for active and passive gears.

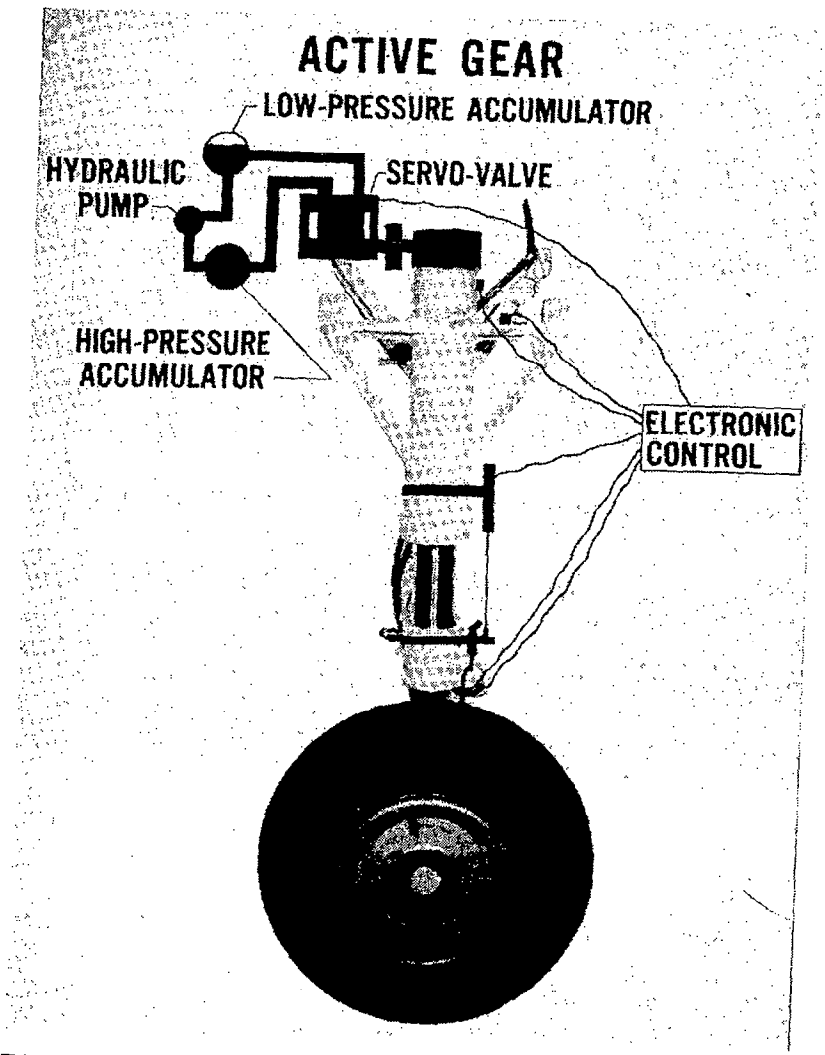

Figure 16.- General aviation aircraft landing gear modified with series-hydraulic active control.